SUPPLEMENTARY INFORMATION

Supplementary Figures and Tables

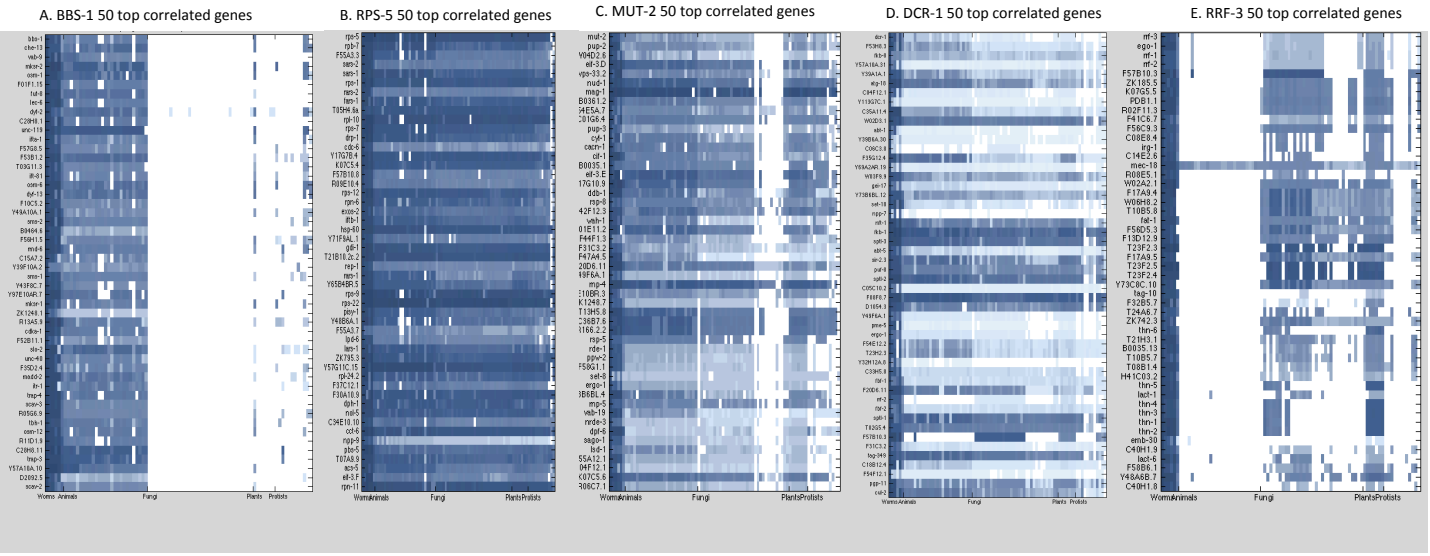

Supplementary Figure 1: phylogenetic profiles of the 50 proteins mostly correlated with: A. BBS-1, B. RPS-5, C. MUT-2, D. RRF-3, E. DCR-1. Correlation coefficients were calculated using the normalized phylogenetic profile matrix (NPP) and genes were rank ordered. Each row represents a gene; dark blue corresponds to high conservation of the *C. elegans* gene in that organism; white denotes no similarity. **A.** A query of the ribosomal S5 protein RPS-5 identifies in the top 30 proteins most correlated in phylogenetic profile 7 other ribosomal proteins with no similarity to RPS-5 as well as 6 tRNA synthetases also involved in translation. The ribosome is one of the most conserved components of the cell; strong conservation across nearly the entire phylogeny correlates the profiles of these proteins. **B.** A query of the ciliated sensory ending component BBS-1 detects the known ciliated ending components CHE-13, MKSR-2, OSM-1, IFTA1, IFT-81, DYF-2, OSM-6, and DYF-13 in the top 20 proteins with a correlated phylogenetic profile, BBS-1 shows no protein sequence similarity to any of these phylogenetically correlated *C. elegans* factors[29]. The driving pattern of this phylogenetic profile correlation is strong conservation in all animals and particular protists, but no homologue in any of the fungi or plants tested.

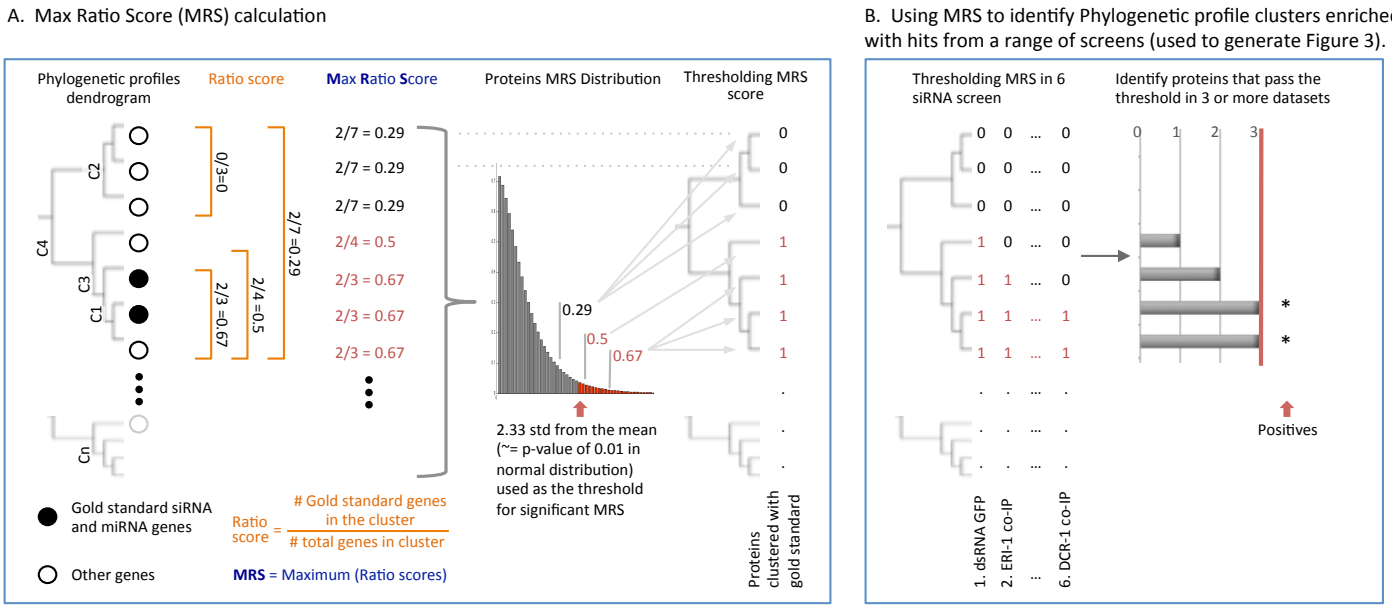

Supplementary Figure 2: Identification of proteins that cluster phylogenetically with known small RNA co-factors or with hits from a set of small RNA genetic and biochemical screens. A. Hierarchical clustering of the NPP was used to cluster the proteins such that each could be assigned to several clusters, ranging from small, tight clusters (i.e. c1, c2) to clusters that contain more members (c3 or the even looser c4). The ratio of the number of validated RNAi pathway proteins to the total number of proteins in each cluster was calculated (termed the ratio score). Because each protein can have several ratio scores, depending on the number of clusters it belongs to, the highest ratio score per protein was used (termed the Maximum Ratio Score (MRS)). To identify those proteins with a significant MRS, we applied a filter, retaining only proteins with MRS ≥ 2.33 Standard Deviations (SD) from the mean (p-value <0.01). **B**. MRS calculation and thresholding was applied to each protein in the six datasets used to identify siRNA cofactors (see Supplementary Methods). Proteins that passed the threshold of 2.33 in at least three of the six datasets were considered positives and reported in Figure 3 (similar analysis was done to identify candidate miRNA pathway proteins).

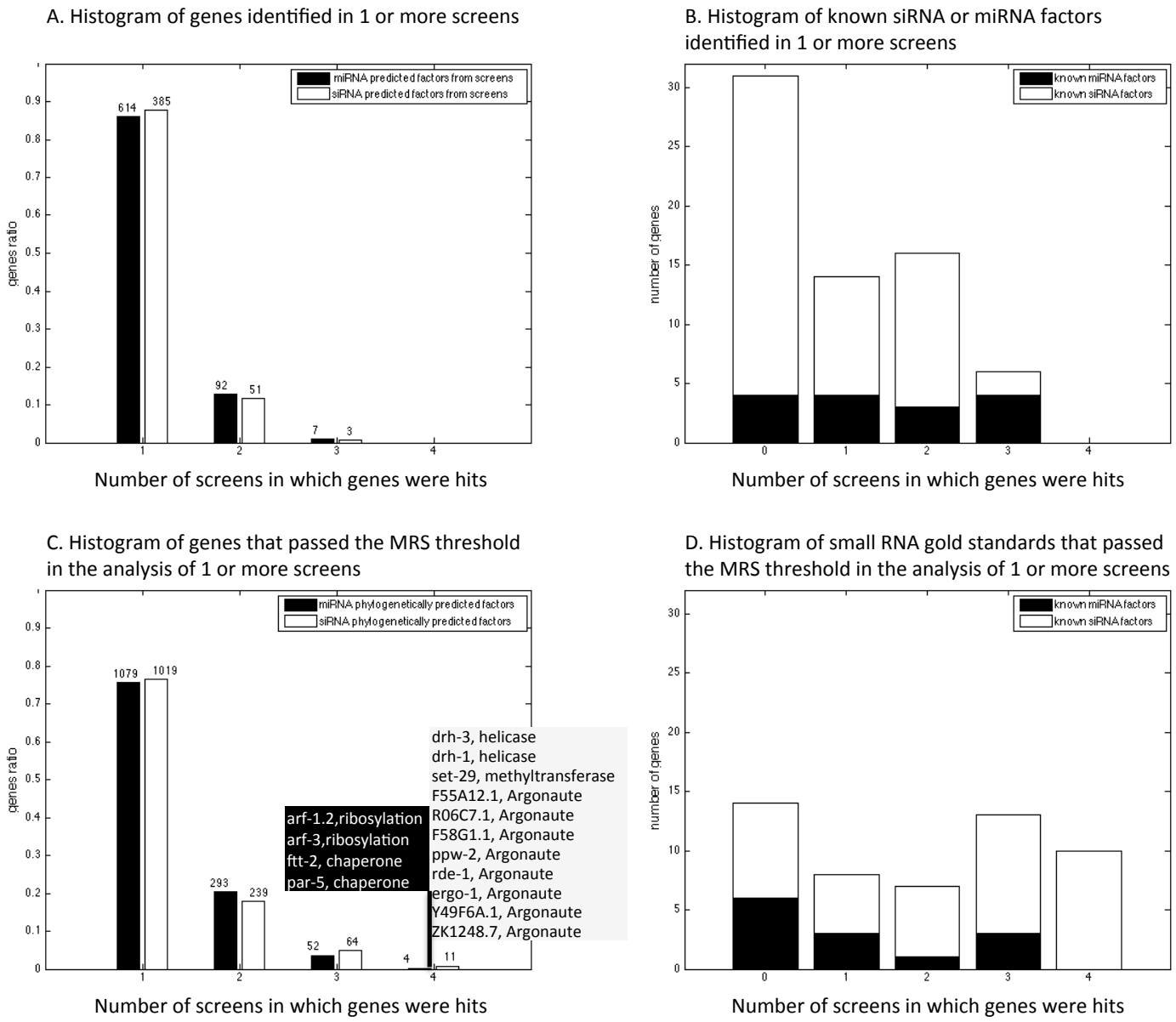

Supplementary Figure 3: Overlap of genes and known small RNA factors between different screens without (A-B) and with (C-D) taking into account the phylogenetic clustering. A. Histogram of proteins that emerged from the siRNA (white) or miRNA (black) screens that were hits in 1, 2, 3, or 4 screens to identify siRNA or miRNA factors (see Methods). Absolute numbers are given above the bars. **B**. The number of previously validated siRNA (white) or miRNA (black) pathway proteins identified as hits in 0 to 4 screens. **C.** Histogram of the ratio of proteins (among those that emerged from the siRNA (white) or miRNA (black) screens) that passed the Max Ratio Score (MRS) threshold (Supplementary Figure 2) in the analysis of 1, 2, 3, or 4 screens. Absolute numbers are given above the bars. **D.** The number of previously validated small RNA pathway proteins that obtained a significant score in the MRS analysis of 0 to 5 screens.

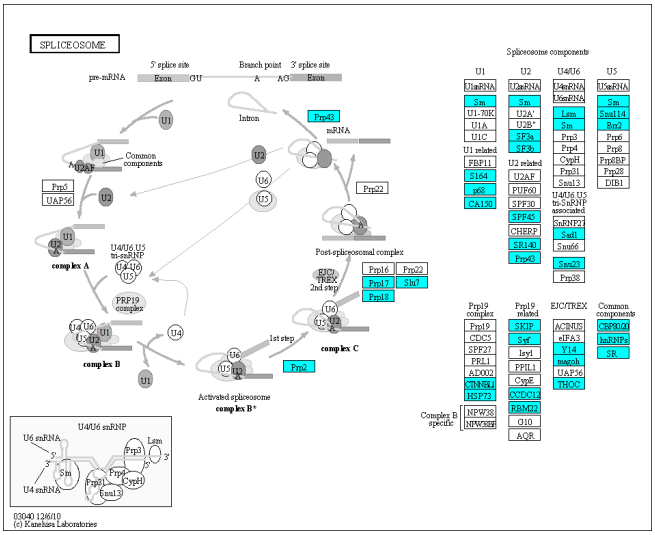

Supplementary Figure 4: **Proteins assigned to the spliceosome by KEGG pathway analysis.** Cyan boxes represent the proteins that received the high scores in the Bayesian classification for siRNA co-factors (Supplementary Table 4), proteins that mapped to the same phylogenetic profile clusters as known small RNA-related factors (Figure 2), or proteins found in clusters enriched with hits from a range of proteomic and functional genomic small RNA screens (Figure 3).

taxonomic group	Organizm	Introns/ gene	Homology to ALG-1
Amoebozoa	Dictyostelium discoideum	**1.2850**	**0.08651801**
Chromalveolata	Theileria parva	2.5804	0
Chromalveolata	Hemiselmis andersenii	0.0000	0
Chromalveolata	Guillardia theta	0.0253	0
Chromalveolata	Plasmodium falciparum	1.4038	0
Chromalveolata	Cryptosporidium parvum	0.0130	0
Protista	Leishmania braziliensis	0.0128	0
Protista	Leishmania infantum	0.0095	0
Protista	Trypanosoma brucei	0.0002	0
Fungi	Cryptococcus neoformans	**5.2729**	**0.182631579**
Fungi	Aspergillus fumigatus	**1.9345**	**0.16**
Fungi	Ustilago maydis	0.7510	0
Fungi	Eremothecium gossypii	0.0479	0
Fungi	Pichia stipitis (Scheffersomyces stipitis)	0.4414	0
Fungi	Encephalitozoon cuniculi	0.0075	0
Fungi	Magnaporthe grisea	1.6766	0
Fungi	Aspergillus niger	**2.5760**	**0.1568326**
Fungi	Gibberella zeae	**2.2235**	**0.1458903**
Fungi	Neurospora crassa	**1.7423**	**0.1481193**
Fungi	Schizosaccharomyces pombe	**0.9367**	**0.2172181**
Fungi	Yarrowia lipolytica	0.1114	0
Fungi	Saccharomyces cerevisiae	0.0553	0
Fungi	Debaryomyces hansenii	0.0526	0
Fungi	Kluyveromyces lactis	0.0244	0
Fungi	Candida glabrata	0.0161	0
Fungi	Malassezia globosa	0.5000	0
Plantae	Micromonas sp. rcc299	**0.5160**	**0.183684211**
Plantae	Ostreococcus lucimarinus	0.2790	0
Plantae	Vitis vinifera	**4.7500**	**0.3458917**
Plantae	Arabidopsis thaliana	**4.1479**	**0.3568341**
Plantae	Oryza sativa	**3.7902**	**0.3517682**
Mammalia	Homo sapiens	**7.7219**	**0.6281633**

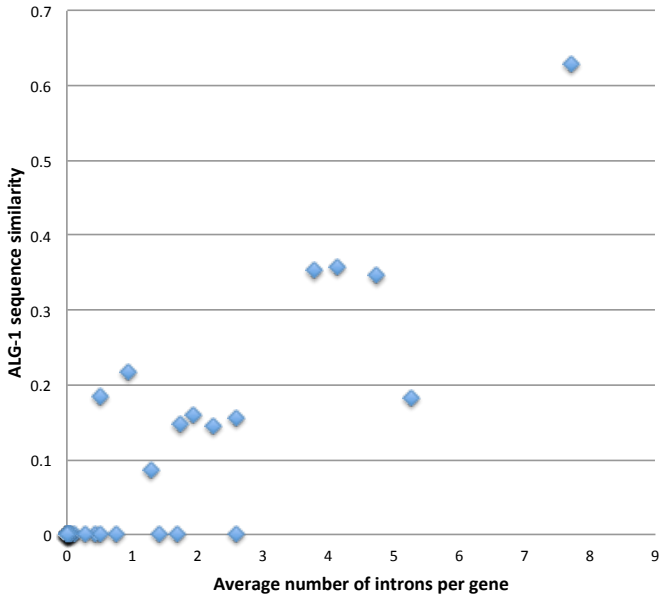

Supplementary Figure 5: Relation between the average number of introns per gene in each species and the presence or absence of Argonaute proteins. Average number of introns per gene were taken from Kaplunovsky et al.[30] and Koralewski et al.[31] (x-axis). Protein similarity to the *C. elegans* ALG-1 was calculated using blastp (see Supplementary Methods). Since all metazoans have many introns and all have conserved Argonaute proteins, we present one representative metazoan, *Homo sapiens*. There is a clear general trend for organisms with more introns to have significant Argonaute homologues. But there are outliers that are not explained by our model: for example, the fungus *Magnaporthe grisea* and the chromalveolate *Theileria parva* have no Argonaute but retain significant intron numbers.

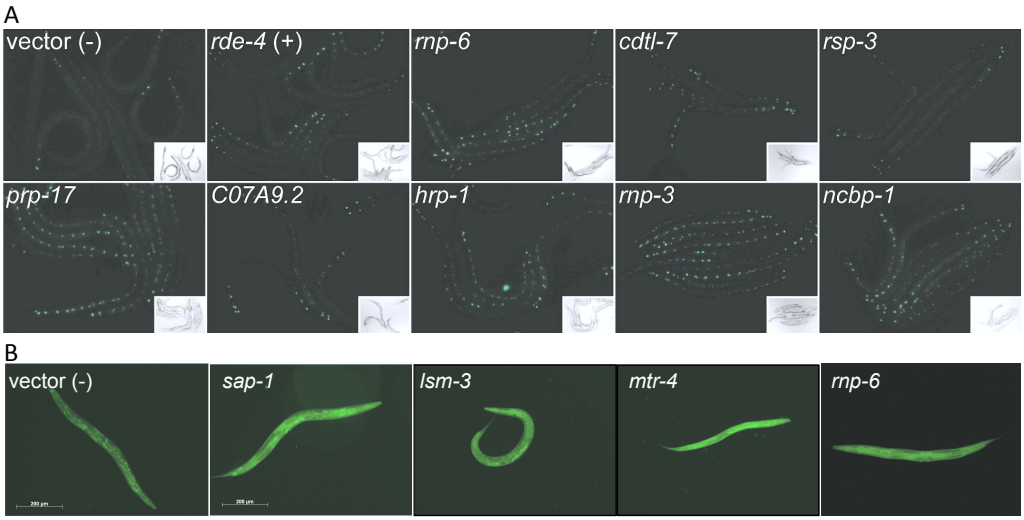

Supplementary Figure 6: Inactivation of splicing factors that are implicated in the RNAi pathways reanimates transgenes targeted by RNAi. A. Expression of *scm::gfp* in the seam cells of an *eri-1(mg366)* mutant, where it is normally silenced by an RNAi pathway. Animals shown were treated with control, *rde-4*, *rnp-6, cdtl-7, rsp-3, prp-17, C0749.2, hrp-1, rnp-3,* or *ncbp-1* RNAi. **B.** GFP expression from the *ubl-1::gfp-siR-1* sensor transgene, which is normally silenced by the siR-1 endogenous siRNA. Animals shown were treated with control, *sap-1*, *lsm-6*, *mtr-4* or rnp-6 RNAi.

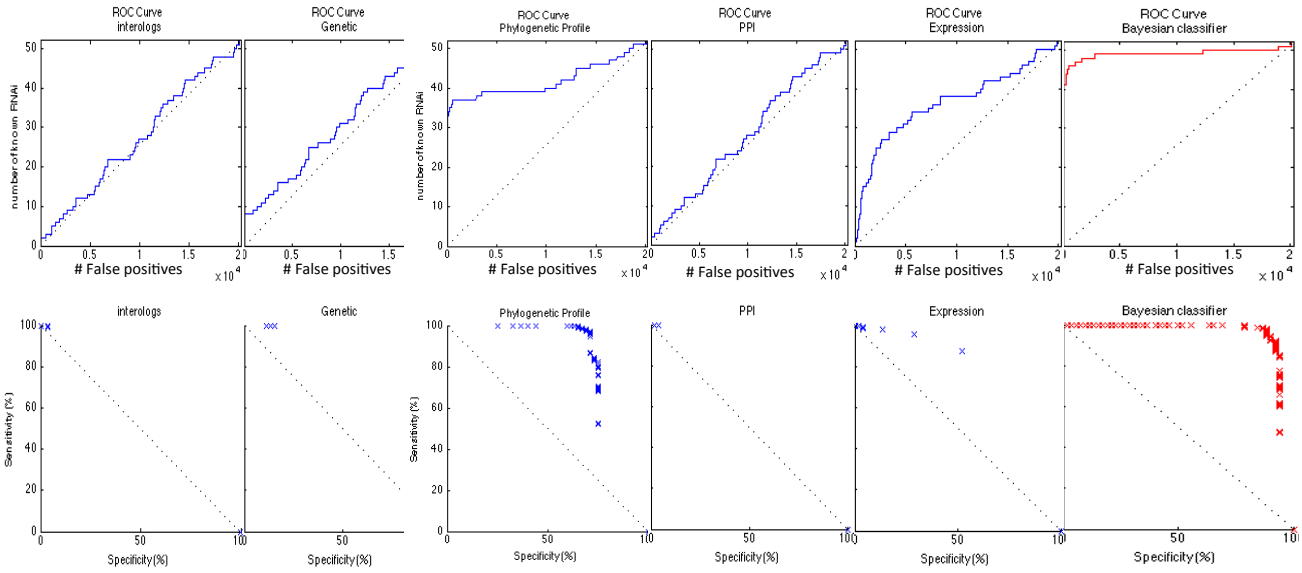

Supplementary Figure 7: Receiver operating characteristic (ROC) analysis. Graphical representation of the Naïve Bayesian Classifier performance (see methods) in discovery of known siRNA factors (in red) compared to single datasets (in blue). For each dataset, a Likelihood Ratio score was calculated and the sensitivity as function of the specificity (Or number of known RNAi factors compared to other genes) was plotted.

Supplementary Table 1: The *C. elegans* phylogenetic profile database. Each row is a blastp bit-score between a single *C. elegans* protein and the top blast hit in each of the 85 other genomes. Among the ~20,000 *C. elegans* proteins, 10,054 are conserved proteins that have homologues (bearing significant protein domain sequence similarity) or orthologues (reciprocal top blast hit in each species) in other eukaryotic genomes. The result is a table of 10,054 proteins X 86 species. The table continues the gene list from Figures 1-3.

Supplementary Table 2: Top siRNA pathway candidates and experimental tests of informatic predictions. Column A-M: Likelihood Ratio score indicating the contribution of being a positive in each of 10 different screens, gene coexpression, or protein-protein interaction to the probability of being a small RNA cofactor relative to baseline (see Supplementary Methods). **Column J-M:** The 87 genes were chosen for further validation based on: high Naïve Bayesian Classifier score, similar phylogenetic profile to RDE-1, similar phylogenetic profile to other known siRNA genes, or high CR score (Figure 1-3). **Column R,S:** score in the *eri-1* transgene desilencing screens**. Column T:** score in the 22G-siR-1 siRNA sensor screen.

Studies	% SiRNA (52)	% MicroRNA (15)	let-7 sensitized	let-7 phenotype	Drosophila miRNA	AIN-2 Co-IP	DCR-1 Co-IP	ERI-1 Co-IP	Drosophila siRNA	ds GFP RNAi	Germline Supression defect	SynMuv supression	Suppression of transgene silencing in eri-1
let-7 sensitized	7.7%	40.0%	319	78	7	3	3	5	11	7	5	1	68
let-7 phenotype	11.5%	33.3%	0	296	7	1	4	6	12	13	5	2	63
Drosophila miRNA	5.8%	33.3%	4E-04	3E-04	71	2	2	4	63	4	0	2	13
AIN-2 Co-IP	1.9%	20.0%	0.034	0.492	0.011	38	6	3	0	0	0	0	1
DCR-1 Co-IP	19.2%	20.0%	0.243	0.078	0.057	5E-08	95	22	3	3	1	1	10
ERI-1 Co-IP	19.2%	20.0%	0.026	0.005	6E-04	0.001	0	89	5	4	1	0	9
Drosophila siRNA	7.7%	20.0%	2E-05	1E-06	0	1	0.028	4E-04	120	6	0	3	23
ds GFP RNAi	23.1%	13.3%	0.001	5E-09	5E-04	1	0.012	0.001	4E-05	90	3	6	66
Germline suppression defect	11.5%	6.7%	0.01	0.008	1	1	0.317	0.312	1	0.006	71	1	11
SynMuv suppression	0.0%	0.0%	0.444	0.104	0.008	1	0.155	1	0.001	1E-08	0.122	31	17
Suppression of transgene silencing in eri-1	26.9%	46.7%	0	0	3E-05	0.846	0.012	0.027	1E-08	0	5E-04	5E-15	829

Supplementary Table 3: Overlap between positives in each of the functional genomic and proteomic screens and with the lists of known siRNA and miRNA pathway proteins. The table presents the percent of the known siRNA and miRNA proteins that were hits in each screen, the number of hits identified in each screen (the gray diagonal), the number of proteins that were also hits in other screens, (upper triangle) and the hyper-geometric p-value for such an overlap (lower triangle).

screens	% Conserved genes	PC score	p-value
let-7 sensitized	82.4%	0.069	0.01181
let-7 phenotype	84.5%	0.055	0.25922
Drosophila miRNA	100.0%	0.154	<0.00001
AIN-2 Co-IP	94.7%	0.084	0.07598
DCR-1 Co-IP	78.9%	0.068	0.12217
ERI-1 Co-IP	79.8%	0.096	0.00658
Drosophila siRNA	98.3%	0.128	<0.00001
ds GFP RNAi	78.9%	0.103	0.00249
Germline Supression defect	62.0%	0.044	0.55185
SynMuv supression	87.1%	0.097	0.05415
Suppression of transgene silencing in eri-1	72.0%	0.064	0.00526
Known RNAi factors	76.6%	0.164	0.00004

Supplementary Table 4: Phylogenetic Clustering of hits from small RNA functional genomic screens. Positives from the RNAi screens for factors in miRNA or siRNA pathway proteins tend to aggregate into phylogenetic profile clusters (column B), with an average of 80% conserved proteins (defined as top hit blastp scores >50 in more than 8 organisms). The Phylogenetic Coherence (PC) score (column C) was calculated for the conserved proteins in each screen to measure similarity among the phylogenetic profiles in a group of proteins (column D) (see Supplementary Methods).

Supplementary Table 5: Top miRNA pathway candidates by Bayesian analysis. To estimate the likelihood of protein *a* being part of the siRNA pathway, we examined its score relative to the scores of the highly validated miRNA proteins in the relevant datasets. This was performed in two stages: First, we computed the likelihood ratio of protein *a* being associated with the miRNA pathway given the evidence from a single dataset (columns F-P). Next, we combined all likelihoods from the individual datasets into one predictive score (column Q).

Supplementary Table 6: RNA interference defects after gene inactivations of *C. elegans* orthologues of known splicing factors. Columns F-H: The scores of gene inactivations of splicing factors with a transgene silenced by one particular endogenous siRNA or a transgene that is desilenced if RNAi is defective. Columns I-R: scores for these same gene inactivations from 10 other full genome screens for small RNA defects. Columns S: if the gene maps to a phylogenetic cluster of a known small RNA factor and the rank of the correlation. Above (in gray) are the p-values that were calculated for over-representation of splicing factors in each of the genome-wide small RNA studies. Gene inactivation of 33 out of 89 splicing factors from the KEGG dataset caused embryonic or early larval arrest that interfered with these tests, so only 46 of the 89 gene inactivations could be tested.

Supplementary Table 7: Genome-wide transgene desilencing screen positives. Roughly 800 RNAi inactivations caused transgene desilencing. Of these, 448 were strong hits (scoring 2 or more). Genes

targeted by positive clones are listed with average score as determined by screening process described in Supplementary Methods and Kim et al. (Kim et al., 2005).

miRNA factors	siRNA Factors			
ain-1	C04F12.1	eri-9	rde-10	tsn-1
ain-2	cgh-1	haf-6	rde-2	vig-1
alg-1	cid-1	mut-14	rde-4	wago-2
alg-2	csr-1	mut-15	rrf-1	wago-4
dcr-1	dcr-1	mut-16	rrf-2	Y49F6A.1
drsh-1	drh-1	mut-2	rrf-3	ZK1248.7
lin-28	drh-3	mut-7	rsd-2	ZK757.2
lin-41	ego-1	ncbp-1	rsd-3	
ncbp-1	ekl-1	ncbp-2	rsd-6	
ncbp-2	ergo-1	nrde-3	sago-1	
nhl-2	eri-1	pir-1	sago-2	
pash-1	eri-3	ppw-1	sid-1	
pup-2	eri-5	ppw-2	sid-2	
xpo-1	eri-6	R06C7.1	T22B3.2	
xrn-2	eri-7	rde-1	T22H9.3	

Supplementary Table 8: The validated siRNA and the miRNA pathway proteins. These genes and their encoded proteins were included in the validated list if the factor has been genetically or biochemically found to be a component of small RNA pathways. Using these criteria, we assembled a list of 52 factors that act in the siRNA pathway and a list of 15 factors that act in the miRNA pathway.

Supplementary Methods

Almost 50% of C. elegans genes encode proteins that are nematode-specific and excluded from this phylogenetic analysis. While the expected trend for conservation of most *C. elegans* proteins correlates with phylogenetic distance, with higher conservation in animals, less conservation in fungi and plants, and even less in protists. However, there are numerous dramatic examples of much higher divergence or even disappearance of homologues in particular clades; we focus on one such example, the small RNA cofactors.

The validated small RNA pathway factors are broadly conserved among RNAi-competent organisms. Furthermore, candidates identified by RNAi screens for small RNA pathway factors are highly enriched for conserved proteins (proteins that have homologous protein outside nematode) , with an average of 80% conserved (Supplementary Table 2), and tend to aggregate into phylogenetic profile clusters (as measured using Phylogenetic Coherence score; see below). This suggests that the analysis captures much of the small RNA pathway despite the exclusion of nematode-specific proteins.

Phylogenetic profile generation

Protein sequences for *C. elegans* were downloaded using BioMart version 0.7 from the Ensembl project (release 60). When different splice variants existed for a gene, the longest variant was used. The

resulting 20,242 protein sequences of C. *elegans* were compared using blastp of all open reading frames (ORFs) of 85 additional organisms. From the existing genomes available in the Ensembl database (release 60), we filtered a set of 53 fully sequenced eukaryotic genomes with no more than one genome per genus (except *Caenorhabditis*). Because Ensembl includes only a limited number of fungi and protists, 33 additional high quality genomes from the NCBI genome database were added to supplement the analysis. The blastp comparison generates a matrix P of size 20,242 x 86 where each entry P_{ab} is the best blastp bit score between a *C. elegans* protein sequence '*a*' and the top result in organism '*b*'. The blastp scores provide a continuous phylogenetic profile, indicating homology level at each species. This approach is more sensitive than traditional binary phylogenetic profiles, which are based only on a comparison of the presence or absence pattern of suites of factors in particular clades of organisms[32,33]

Preprocessing and clustering the phylogenetic profiles

Preprocessing and normalization were applied to the profile matrix P prior to clustering. We used a preprocessing approach similar to that described by Enault et al.[34], related to the original binary phylogenetic profile preprocessing[32].

Our method included several steps that were performed on the phylogenetic profile matrix P:

1. Thresholding low blastp bit scores: To reduce the influence of random matches in the phylogenetic profiles, low blastp bit scores (<50) were assigned a value of 1 (if P_{ab} <50 then we set P_{ab} =1).

2. Excluding poorly conserved proteins from the phylogenetic analysis: We have excluded proteins with less than five orthologues in the 81 non-nematode organisms from further phylogenetic analysis, since calculating the correlation between poorly conserved proteins is mainly governed by the zeros (no homologue found) across the phylogenetic matrix, and therefore such correlation measurement is likely less reliable.. From a total of 20,242 worm proteins, only 10,054 passed this filter and were used for the subsequent phylogenetic profiling analysis.

3. Normalizing the blastp bit scores for protein length: Since the blastp score depends linearly on the length of protein '*a'*, long alignments would tend to have higher scores independently of whether the aligned segments show sequence similarity, resulting a bias towards longer proteins. We therefore next normalized the phylogenetic profile matrix values to remove biases resulting from variations in protein lengths. In addition to P_{ab}, the best blastp bit score between a *C. elegans* protein *a* and all ORFs of a eukaryote genome '*b'*, we computed P_{aa}, defined as the self-similarity score of the *C. elegans* protein '*a'* when blasted against itself. In LenNPP, the normalized phylogenetic profile matrix, each entry in the row corresponding to protein '*a'* is computed as: $LenNPP_{ab} = \log_2(P_{ab}/P_{aa})$. The normalized blastp score represents the (log)- ratio of the observed blastp score and the best possible blastp score of the same length (the self-similarity score), thus eliminating dependence on alignment length[34].

4. Normalizing for organisms with different evolutionary distance: A second normalization procedure was applied in order to compensate for the different protein similarity (i.e. score) expected when *C. elegans*

proteins are compared to proteins from eukaryotes of highly variable evolutionary distance. For this purpose we normalized the values in each column *b* (i.e. each organism) by subtracting their average μ_b and dividing by their standard deviation σ_b, yielding:

$NPP_{ab} = (LenNPP_{ab} - \mu_b) / \sigma_b$

The normalized matrix NPP was used for subsequent clustering analysis.

For the more global clustering of proteins, a phylogenetic profile correlation (R) was calculated for each pair of the 10,054 proteins in the dataset. These R-values were used to cluster the proteins by average linkage, yielding groups of proteins with similar phylogenetic profiles.

Phylogenetic Coherence score

To measure if a particular set of proteins tends to have a more similar phylogenetic profile than a random set of genes, we have developed the Phylogenetic Coherence (PC) score. The PC score measures how close on average are the phylogenetic profiles of proteins within a set compared to within a random set of proteins. A high PC score indicates that proteins within a set show similar phylogenetic profiles, a characteristic known to be associated with similar function[32,33,35]. The PC score is a variation of the Expression Coherence (EC) score, which was originally developed to measure how similar a set of proteins is with regard to their expression profiles across different conditions[36,37].

To calculate the PC score for a given set A of K genes, the Pearson correlation between the normalized phylogenetic profiles (the NPP matrix) of each of the K x (K - 1) / 2 pairs of proteins in A was calculated. The phylogenetic coherence score is simply defined as the fraction of pairs whose score exceeds a threshold, PC(A) = p(A,S) / (K(K - 1) / 2)), where p(A,S) is the number of gene pairs in set A whose phylogenetic similarity is better than a threshold similarity S. We determined the value of the threshold S as follows: We calculated the Phylogenetic correlation between all 10,057 conserved *C. elegans* protein sequence pairs (10,054 x 10,053 / 2 = 50,536,431) and then defined S as the 95th percentile of the distribution of these similarities (such that a random set of K sequences should get, on average, a PC score of ~0.05). If the sequences in our set K tend to have more similar phylogenetic profiles than a random set, their PC score should be > 0.05.

To assign a p-value for the PC score of a list of sequences A of size K, the process was repeated 10,000 times for random sets of sequences of the same size K. PC scores were calculated for the random sets and used to rank of the true set's score PC (A) among the 10,000 randomized scores, yielding an empirical p-value for the PC score of the true set A. Finally, to test the robustness of the method to the threshold choice, alternative thresholds (S) were tested. These yielded similar p-values and identified similar factors as significant (data not shown).

The validated siRNA and the miRNA pathway factors

To identify new proteins that are part of small RNA pathways, we compiled two gold standard lists of factors with evidence in the literature for a role in either the siRNA or miRNA pathway. A factor was included in a gold standard list if the factor has been genetically or biochemically found to be a component of the small RNA pathways. Using these criteria, we assembled a gold standard list of 52 factors that are part of the siRNA pathway and a list of 15 factors that are part of the miRNA pathway (see lists in Supplemental table 8). Three factors, DCR-1, NCBP-1, and NCBP-2, are in both lists. The average linkage method produces a hierarchical clustering (dendrogram), and distinct clusters were obtained by 'cutting' the dendrogram at various thresholds, producing different numbers of clusters.

The Cluster Ratio and Max Ratio Scores

Given a pre-defined set of proteins of interest $G_{interest}$ (for example, proteins with shared biological function such as the siRNA pathway factors, or factors obtained as results of a certain biological assay such as an RNAi screen), we wanted to identify which other *C. elegans* proteins might be related to this set based on similarity in their phylogenetic profiles. For this purpose, we have clustered the NPP and used the obtained dendrogram to score proteins for phylogenetic similarity with the list of validated factors. The dendrogram was thresholded to obtain N distinct clusters using the MATLAB 'cluster' function, for different clustering resolutions N. Next, we looked for each factor *a* at the overlap between the cluster to which it was assigned $G_{cluster(a,N)}$ and the list of factors of interest $G_{interest}$. To quantify this overlap, we have calculated for each factor *a* the Cluster Ratio (CR) score $CR_{a,N}$, which is the fraction of factors from the cluster $G_{cluster(a)}$ that belong to the list of interest ($G_{interest}$).

$CR_{a,N} = |G_{interest} \cap G_{cluster(a,N)}| / |G_{cluster(a,N)}|$

Where here |A| denotes the number of factors in a set A. (see supplementary fig 2 showing the cluster ratio score)

The CR score captures the tendency of factors to appear together with the list of interest based on the clustering dictated by our dendrogram, with factors having a high CR score showing similar phylogenetic profile to one or several factors in our list of interest. Such genes represent candidate factors predicted to have similar function with our list of validated miRNA and siRNA pathway factors.

For the phylogenetic profile of each factor *a*, we have tested the similarity to the profiles of factors on the list of interest at various similarity levels by modifying the clustering resolution. This was achieved by altering the number of clusters N obtained from the dendrogram, with N values chosen to be N = 10,50,100, 200,…., 9000, 10000. This resulted in 102 different Cluster Ratio ($CR_{a,N}$) scores for each factor *a*. Finally, for each factor we chose the clustering resolution maximizing the cluster ratio, giving us the gene's Max Ratio Score: $MRS_a = \max (CR_{a,10}, CR_{a,50},.., CR_{a,10000})$; when cluster is define as a group of 3 or more proteins with most similar profile to each other. The MRS for each factor *a* represents the optimized phylogenetic clustering resolution achieving the highest enrichment for factors of interest in a cluster containing gene *a*.

Integration of genome-scale data sets

Sixteen recently published studies and genome-wide databases were integrated using a Naïve Bayesian Classifier (see below) to predict new factors that are part of the siRNA or miRNA pathways. From the 16 datasets described below, 12 were used to predict new factors in the siRNA pathway and 11 were used to predict new factors in the miRNA pathway, as indicated below:

***let-7* sensitized background screen (miRNA):** The *let-7* miRNA is conserved in other organisms[38,39]. A sensitized background of a weak *let-7* allele, *mg279*, was used to identify miRNA pathway factors by genome-wide RNAi screening for enhancement of the *let-7(mg279)* vulval rupture phenotype[40]. Screen positives were divided into three categories: weak, medium, and strong. From the total of 332 hits in the screen, 105 were not repeated in a secondary screen and considered as weak hits (we scored them 1), 169 genes retested positive in triplicate, considered as a medium hits (scored 2), and 45 were validated by genetic tests and declared strong hits (scored 3). Three genes didn't match our gene database, and all the other genes in the database were scored 0.

Vulval bursting phenotype screen (miRNA): The *let-7* miRNA controls the L4-to-adult transition. *let-7* mutants fail to execute this transition and die by bursting through the vulva [39]. This vulval bursting phenotype can therefore indicate defects in miRNA pathway function. We have downloaded from WormBase (WS220) a list of 296 genes with the exploded through vulva phenotype in RNAi experiments. These genes were scored 1 to indicate a vulval bursting phenotype, and all other genes were scored 0.

***D. melanogaster* miRNA type (imperfect duplex) 3' UTR reporter screen (miRNA):** A genome-wide RNAi screen was performed in *D. melanogaster* S2 cells to identify factors that impact miRNA pathway function[41]. *C. elegans* orthologues of tested protein sequences were scored 1 if positive, 0 if not. *C. elegans* proteins whose orthologues were not tested were assigned a null score.

AIN-2 Co-immunoprecipitation (miRNA): AIN-2 interacts with miRNA-specific Argonaute proteins and regulates the expression of miRNA targets. To identify proteins interacting with AIN-2, which could represent miRNA pathway factors, a mass spectrometry-based proteomics approach was applied [42]. The 38 identified AIN-2-interacting factors were scored 1, and all others were scored 0.

DCR-1 Co-immunoprecipitation (siRNA and miRNA): A mass spectrometry-based proteomics approach was used to identify DCR-1-interacting proteins[43]. The purification process was performed in duplicate under native conditions in embryos and gravid adults [43]. We scored as follows: Proteins identified in mass spectrometry of DCR-1 complexes in both embryonic and adult purifications received a score of 2. Proteins identified in two repeats of a single purification (embryonic or adult) received a score of 1. Otherwise, proteins were scored according to the peptide coverage ratio, which was always less than one (i.e. for peptide coverage of 26%, the gene score is 0.26).

ERI-1 Co-immunoprecipitation (siRNA): A mass spectrometry-based proteomics approach was used to identify ERI-1-interacting proteins. A tagged ERI-1 protein was purified using standard protein biochemistry

under native conditions, washed extensively, and interacting proteins were identified by mass spectroscopy. The ERI-1-interacting factors were scored 1, and all others were scored 0.

***D. melanogaster* siRNA type (perfect duplex) 3' UTR reporter screen (siRNA):** A genome-wide RNAi screen was performed in *D. melanogaster* S2 cells to identify genes that impact siRNA pathway function [41]. *C. elegans* genes orthologous to tested genes were scored 1 if positive, 0 if not. *C. elegans* genes whose orthologues were not tested were assigned a null score..

Transgene RNAi screen (siRNA): A genome-wide RNAi screen was performed in an engineered RNAi sensor strain of *C. elegans* to identify genes required for RNAi. Genes corresponding to the RNAi clones were scored on a GFP intensity and penetrance scale of 0 (no GFP expression) to 4 (highly penetrant, strong GFP expression), and those that scored an average of 2 or greater were designated candidate RNAi genes[44]. We used numerical scores as reported in the paper.

Germline cosuppression defect screen (siRNA): During silencing of repetitive transgenes, a trans effect ("cosuppression") occurs that results in silencing of cognate endogenous genes. A genome-wide RNAi screen was performed in an engineered germline cosuppression sensor strain of *C. elegans* to identify factors required for cosuppression in the germline[45]. Positives were scored 1, and all others were scored 0.

Suppression of synMuvB and synMuvA synthetic multivulva (Muv) phenotype screen (siRNA): SynMuv B genes are involved in multiple cellular functions during development including RNA interference [46]. A genome-wide RNAi screen was performed in the *lin-15AB(n765)* background to identify suppressors of the Muv phenotype [46]. SynMuv suppressor genes were scored 1, and all others were scored 0.

Phylogenetic profiling analysis (siRNA and miRNA): We have generated phylogenetic profiles for the entire worm proteome by blastp, searching all ~20,000 worm proteins across all 86 genomes (see Methods, above). Proteins were clustered based on phylogenetic profile similarity, and the score used for each is the Max Ratio score (MR) (see Methods, The Cluster Ratio and Max Ratio scores).

Co-expression analysis (siRNA and miRNA): For each gene in the gold standard groups (siRNA or miRNA) we identified, using the SPELL engine (Serial Pattern of Expression Levels Locator) [47], the 100 genes that correlate best in 72 different gene expression data sets. The results are 100 x 51 (for the siRNA) and 100 x 14 (for the miRNA) tables of the most correlated genes for each of the gold standard genes. For each gene, independent siRNA and miRNA co-expression scores were calculated as the number of time the gene is found in each of the tables (e.g. *inx-22* was among the top 100 co-expressed genes of 15 of the siRNA and 2 of the miRNA gold standard factors; hence, its scores are 15 for siRNA and 2 for miRNA).

Protein-protein interactions: A genome-scale protein-protein interaction map generated from yeast two-hybrid data was downloaded from the Worm Interactome version 8[48]. We scored each gene by calculating the ratio of its number of interactions with the siRNA or miRNA gold standard factors to its total number of interactions.

Interologs: protein-protein interactions of orthologues of C. *elegans* protein coding genes: Predicted pairs of C. *elegans* interactors whose respective orthologues were experimentally shown to interact in another

organism were downloaded from Worm Interactome version 8 [48]. We scored each factor by calculating the ratio of its number of interactions with the siRNA or the miRNA gold standard factors to its total number of interactions.

Predicted genetic interactions from text mining: WormBase provides a list of genetic interactions that are text processed and manually curated[48]. We scored each gene by calculating the ratio of its number of interactions with the siRNA or the miRNA gold standard factors to its total number of interactions.

Gross phenotypic signatures: A list of genes pairs that share phenotypic similarity were download from the Worm Interactome version 8[48]. We scored each gene by calculating the ratio of its number of pairings with the siRNA or the miRNA gold standard factors to its total number of pairings.

For each of the two pathways, the entire dataset was represented by one data matrix D, where D_{ab} represents the value obtained for factor '*a'* in dataset *b*. Values were either binary (e.g. for the vulval bursting phenotype screen), or quantitative (e.g. for the protein-protein interaction dataset). In all datasets, higher values suggest a higher probability of a factor belonging to the siRNA or miRNA pathways.

For brevity, we describe here the analysis for the siRNA pathway. The miRNA pathway analysis is identical, except for a different gold standard set and data matrix D used. To estimate the likelihood of factor '*a'* being part of the siRNA pathway, we examined its score relative to the scores of the gold standard genes in all datasets. This was performed in two stages: First, we computed the likelihood of factor '*a'* being associated with the siRNA pathway given the evidence from a single dataset. Next, we combined all likelihoods from the individual datasets into one predictive score. For the true status of factor '*a*' is marked by a binary variable Y_a, which is equal to one if the factor is part of the siRNA pathway. Since we don't know if factor *a* is part of the siRNA pathway, Y_a is unknown, and our goal is to predict it as accurately as possible, given the dataset D. Methods are defined in the following sections.

A screen that is useful for our analysis is indicated by scores for the gold standard factors that are higher than expected by chance. Therefore, a factor getting a high score is more likely to function in the siRNA pathway. We utilized this information to define a likelihood ratio score as follows: For each factor *a* in each dataset *b*, we defined a threshold score t_{ab}, such that all factors with scores in the dataset greater or equal to this threshold are considered positives, and other factors are considered negatives. For binary traits, the threshold t_{ab} was simply chosen to be $t_{ab} = D_{ab}$, such that positives are either all factors with score '1' (in case factor '*a'* got a '1' score, giving evidence for it being part of the siRNA pathway) or all factors (in case factor '*a'* got a '0', offering no evidence for pathway membership). For quantitative datasets, threshold selection was slightly more complex. The use of D_{ab} as a threshold might be sub-optimal and even misleading - this is particularly true in cases when D_{ab} is very high and none of the gold standard factors passed D_{ab}. We therefore examined all thresholds $t \leq D_{ab}$ and calculated the likelihood ratio $LR_{ab}+(t)$ for each possible threshold (as described below). We then set the threshold t_{ab} as the one maximizing the obtained likelihood ratio, and took

$LR_{ab}+ = MAX_t\{LR_{ab}+ (t)\}$.

Once a threshold has been set, we have computed a Likelihood Ratio score $LR_{ab}+$, a measure of a test power indicating how the knowledge of a specific score changes the likelihood of a factor being part of the siRNA pathways from baseline. More precisely, the likelihood ratio score is defined as $LR_{ab}+ = Pr(Y_a = 1 \mid D_{ab}) / Pr(Y_a = 0 \mid D_{ab})$; i.e. $LR_{ab}+(t)$ is the ratio of probabilities of a factor *a* being part of the siRNA pathway versus not being part of this pathway given the evidence provided by dataset *b*. For each dataset we set $LR_{ab}+$ as $LR_{ab}+(t)$ using the threshold t chosen as above. In practice, it is computed by comparing the proportion of gold standard factors among the positives (genes which scored above the threshold t_{ab}) and negatives (factors scoring below the threshold), as detailed below.

The value $Pr(Y_a = 1 \mid D_{ab})$ is also often termed sensitivity, and the value $Pr(Y_a = 0 \mid D_{ab})$ is known as one minus the specificity. The sensitivity and specificity values for a given score D_{ab} are defined as:

where:

(i) TP_{ab} denotes True Positives, the number of gold standard factors with scores equal to or higher than the score threshold t_{ab}

(ii) TN_{ab} denotes True Negatives, the number of non-gold standard factors with scores lower than the score threshold t_{ab}.

(iii) FP_{ab} denotes False Positives, the number of non-gold standard factors with scores equal to or higher than the score threshold t_{ab}.

(iv) FN_{ab} denotes False Negatives, the number of gold standard factors with scores lower than the score threshold t_{ab}.

The likelihood ratio, computed via sensitivity and specificity is then given by:

$$specificity = \frac{TN_{ab}}{TN_{ab} + FP_{ab}} = \frac{TrueNegatives}{TrueNegatives + FalsePositives}$$

$$sensitivity = \frac{TP_{ab}}{TP_{ab} + FN_{ab}} = \frac{TruePositives}{TruePositives + FalseNegatives}$$

Finally, we used a Naïve Bayesian Classifier to merge the $LR_{ab}+$ scores from the different datasets and assign a final score. Naïve Bayesian Classifiers provide a simple, standard, and scalable method for utilizing the power of different data sources and types for prediction by assuming conditional independence of the various predictors given the outcome. It has been used successfully in various genomics applications [49-51] and was used here to predict likelihood of membership in the siRNA pathway for a given factor.

We define the final score for a factor '*a*' (S_a) as the log likelihood ratio of the probability of factor *a* being in the siRNA pathway to the probability of factor '*a*' not being in the pathway given evidence collected from all 12 datasets used for the siRNA classifier:

$S_a = \log(Pr(Y_a = 1 \mid D_{a1}, D_{a2},.., D_{a12}) / Pr(Y_a = 0 \mid D_{ab}, D_{a2},.., D_{a12}))$

An underlying assumption of the Naïve Bayesian procedure is that the individual data sets are independent of each other. As such, we can compute S_a by simply summing the log-likelihood ratios:

$S_a = \Sigma_b (LR_{ab}+)$

where $LR_{ab}+$ is the likelihood ratio score of factor '*a'* in data set *b*.

The independence assumption is rarely strictly satisfied in practice[49] Hence treating the dataset as independence may be sub-optimal. Nevertheless, we used the Naïve Bayesian model for two reasons: first, our goal in this work was to show that combining different data sources in a simple manner enables us to reliably predict new siRNA pathway factors; and second, reliably estimating and exploiting the dependencies in our databases is difficult, and often requires larger amounts of data. Better modeling of the dependencies between the different data sources will likely lead to even better classifiers and thus more accurate prediction of gene membership in the pathway.

Validation screens

A transgene that expresses GFP in the hypodermal cells in wild type is silenced in an *eri-1(mg366)* mutant, but RNAi targeting of genes encoding validated small RNA pathway cofactors such as *rde-1*, *rde-4*, or *dcr-1* causes transgene desilencing. *wIs54(scm:gfp)* in *eri-1(mg366)* is silenced in seam cells[44]. Desilencing of the *wIs54(scm:gfp)* transgene in the *eri-1(mg366)* mutant and desilencing of the *ubl-1::GFP::siR-1* endo siRNA sensor transgene was tested in two samples of each of 87 gene inactivations and scored 4 for most desilencing to 0 for least. For the 87 top ranked genes from the Bayesian analysis tested, the sequences of the gene inactivating dsRNAs were verified. In the full genome screen with the *wIs54* in *eri-1(mg366)*, every gene knockdown that caused in any degree of desilencing (score > 0) in the primary screen was subjected to secondary screening in triplicate, scoring 4 for the most desilencing down to 0 for no desilencing. Due to the large number of positives emerging from the full genome screen, plasmids for RNAi clones were not re-sequenced.

Images

Images were captured using a Zeiss Axioplan microscope equipped with a Hamamatsu digital camera and Zeiss Axiovision software. Images compared to each other were captured using the same exposure settings and processed identically. Control RNAi bacteria expressed double-stranded RNA homologous to no worm gene.

REFFERANCES

29 Inglis, P. N., Blacque, O. E. & Leroux, M. R. Functional genomics of intraflagellar transport-associated proteins in C. elegans. *Methods Cell Biol* **93**, 267-304, doi:S0091-679X(08)93014-4 [pii]
10.1016/S0091-679X(08)93014-4 (2009).

30 Kaplunovsky, A., Ivashchenko, A. & Bolshoy, A. Statistical analysis of exon lengths in various eukaryotes. *Open Access Bioinformatics* **2011:3**, 1 - 15, doi:http://dx.doi.org/10.2147/OAB.S14448 (2011).

31 Koralewski, T. E. & Krutovsky, K. V. Evolution of exon-intron structure and alternative splicing. *PLoS One* **6**, e18055, doi:10.1371/journal.pone.0018055 (2011).

32 Pellegrini, M., Marcotte, E. M., Thompson, M. J., Eisenberg, D. & Yeates, T. O. Assigning protein functions by comparative genome analysis: protein phylogenetic profiles. *Proc Natl Acad Sci U S A* **96**, 4285-4288 (1999).

33 Avidor-Reiss, T. *et al.* Decoding cilia function: defining specialized genes required for compartmentalized cilia biogenesis. *Cell* **117**, 527-539, doi:S009286740400412X [pii] (2004).

34 Enault, F., Suhre, K., Abergel, C., Poirot, O. & Claverie, J. M. Annotation of bacterial genomes using improved phylogenomic profiles. *Bioinformatics* **19 Suppl 1**, i105-107 (2003).

35 Pagliarini, D. J. *et al.* A mitochondrial protein compendium elucidates complex I disease biology. *Cell* **134**, 112-123, doi:S0092-8674(08)00768-X [pii]
10.1016/j.cell.2008.06.016 (2008).

36 Pilpel, Y., Sudarsanam, P. & Church, G. M. Identifying regulatory networks by combinatorial analysis of promoter elements. *Nat Genet* **29**, 153-159, doi:10.1038/ng724
ng724 [pii] (2001).

37 Tabach, Y. *et al.* The promoters of human cell cycle genes integrate signals from two tumor suppressive pathways during cellular transformation. *Mol Syst Biol* **1**, 2005 0022, doi:msb4100030 [pii]
10.1038/msb4100030 (2005).

38 Pasquinelli, A. E. *et al.* Conservation of the sequence and temporal expression of let-7 heterochronic regulatory RNA. *Nature* **408**, 86-89, doi:10.1038/35040556 (2000).

39 Reinhart, B. J. *et al.* The 21-nucleotide let-7 RNA regulates developmental timing in Caenorhabditis elegans. *Nature* **403**, 901-906, doi:10.1038/35002607 (2000).

40 Parry, D. H., Xu, J. & Ruvkun, G. A whole-genome RNAi Screen for C. elegans miRNA pathway genes. *Curr Biol* **17**, 2013-2022, doi:S0960-9822(07)02155-0 [pii]
10.1016/j.cub.2007.10.058 (2007).

41 Zhou, R. *et al.* Comparative analysis of argonaute-dependent small RNA pathways in Drosophila. *Mol Cell* **32**, 592-599, doi:S1097-2765(08)00734-X [pii]
10.1016/j.molcel.2008.10.018 (2008).
42 Zhang, L. *et al.* Systematic identification of C. elegans miRISC proteins, miRNAs, and mRNA targets by their interactions with GW182 proteins AIN-1 and AIN-2. *Mol Cell* **28**, 598-613, doi:S1097-2765(07)00626-0 [pii]
10.1016/j.molcel.2007.09.014 (2007).
43 Duchaine, T. F. *et al.* Functional proteomics reveals the biochemical niche of C. elegans DCR-1 in multiple small-RNA-mediated pathways. *Cell* **124**, 343-354, doi:S0092-8674(05)01394-2 [pii]
10.1016/j.cell.2005.11.036 (2006).
44 Kim, J. K. *et al.* Functional genomic analysis of RNA interference in C. elegans. *Science* **308**, 1164-1167, doi:1109267 [pii]
10.1126/science.1109267 (2005).
45 Robert, V. J., Sijen, T., van Wolfswinkel, J. & Plasterk, R. H. Chromatin and RNAi factors protect the C. elegans germline against repetitive sequences. *Genes Dev* **19**, 782-787, doi:gad.332305 [pii]
10.1101/gad.332305 (2005).
46 Cui, M., Kim, E. B. & Han, M. Diverse chromatin remodeling genes antagonize the Rb-involved SynMuv pathways in C. elegans. *PLoS Genet* **2**, e74, doi:10.1371/journal.pgen.0020074 (2006).
47 Hibbs, M. A. *et al.* Exploring the functional landscape of gene expression: directed search of large microarray compendia. *Bioinformatics* **23**, 2692-2699, doi:btm403 [pii]
10.1093/bioinformatics/btm403 (2007).
48 Simonis, N. *et al.* Empirically controlled mapping of the Caenorhabditis elegans protein-protein interactome network. *Nat Methods* **6**, 47-54 (2009).
49 Calvo, S. *et al.* Systematic identification of human mitochondrial disease genes through integrative genomics. *Nat Genet* **38**, 576-582, doi:ng1776 [pii]
10.1038/ng1776 (2006).
50 Jansen, R. *et al.* A Bayesian networks approach for predicting protein-protein interactions from genomic data. *Science* **302**, 449-453, doi:10.1126/science.1087361
302/5644/449 [pii] (2003).
51 Grossman, S. R. *et al.* A composite of multiple signals distinguishes causal variants in regions of positive selection. *Science* **327**, 883-886, doi:science.1183863 [pii]
10.1126/science.1183863 (2010).